

Calculations for the optical system for the first ITER plasma

Burkhard Plaum^{1*}, Mélanie Preynas², and Munseok Choe²

¹Institut für Grenzflächenverfahrenstechnik und Plasmatechnologie, Universität Stuttgart, Pfaffenwaldring 31, D-70569 Stuttgart, Germany

²ITER Organization, Route de Vinon-sur-Verdon - CS 90 046 - 13067 St Paul Lez Durance Cedex - France

Abstract. A dedicated optical system is designed for the breakdown of the first ITER plasma, when the machine will not be equipped with the equatorial ECRH-launcher. Seven beams from the upper launcher will be transmitted via several in-vessel mirrors through the resonance layer to a beam-dump. The whole system was simulated with the PROFUSION package to obtain the beam parameters, estimate spill-over effects and determine the required polarization in the launcher in order to have X-mode polarization in the resonance.

1 Introduction

For the first plasma experiments in ITER, the machine will not be equipped with all components. In particular the equatorial launcher, which is foreseen for central EC-heating, will not be available. This means that for the initial plasma breakdown the upper launcher [1] has to be used.

Since the resonance is near the plasma axis, where the magnetic field lines are mostly in toroidal direction, the microwave needs to cross the resonance with vertical polarization mostly in the horizontal plane in order to heat in X-mode (See Fig. 1). This requires a dedicated optics system [2,3]. In the first version, it contained a grating, which was, however, not feasible due to the extreme angles (shallow incidence, almost perpendicular reflection). A new design consisting only of smooth mirrors was simulated and analysed in this paper.

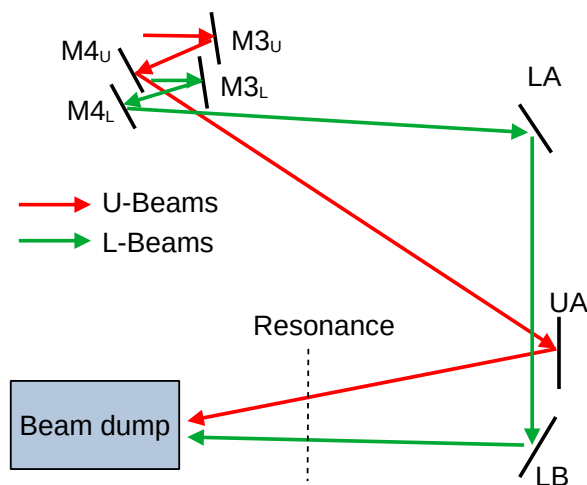


Fig. 1. Beam path of the from the launcher to the beam dump

For the initial plasma breakdown the beams of 7 gyrotrons (1 MW each) will be used. The 3 beams launched by the upper row of the launcher are denoted U1, U2 and U3 respectively. The beams coming from the lower row are denoted L1-L4.

For the upper beams, the steering mirror (M4) in the launcher will be modified with a cylindrical surface, and a common in-vessel mirror (UA) is used to direct the beams towards the resonance.

The lower beams are directed via one common ellipsoidal in-vessel mirror (LA) and four individual hyperboloid mirrors (LB) towards the resonance.

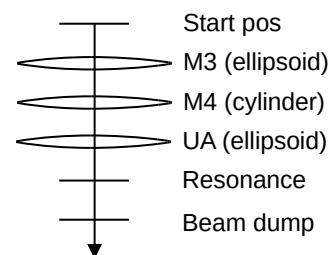


Fig. 2. Beam path of the U-beams from the launcher to the beam dump

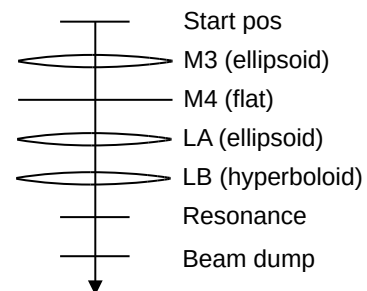


Fig. 3. Beam path of the L-beams from the launcher to the beam dump

* Corresponding author: burkhard.plaum@igvp.uni-stuttgart.de

Figures 2 and 3 show the calculation schemes for the U- and L-beams respectively, where focusing elements are drawn as lenses.

The calculations were done with the PROFUSION code [4], which was extended for this project.

2 Calculation methods

2.1 Physical Optics

The calculation starts inside the upper launcher at a location after the mirror M2, where the beams have a nearly circular shape with a known waist radius. The analytical description is used to generate the incident field on the first mirror.

The reflection is calculated using a physical optics algorithm. It divides the mirror surface into small ($< \lambda/2$) elements. On each of the elements the surface current \vec{J} is calculated from the incident magnetic field and the local normal vector n of the mirror surface under the assumption of a perfect electric conductor:

$$\vec{J} = 2 \vec{n} \times \vec{H}_i \quad (1)$$

From the surface currents, the magnetic field H_r of the reflected beam can be calculated using the Green function of free space:

$$\vec{H}_r = \iint \left(-jk - \frac{1}{R} \right) \vec{J} \times \frac{\vec{R}}{R} \frac{e^{-jkR}}{4\pi R} dx dy \quad (2)$$

where R is the vector from the mirror point to the location, where H_r is calculated, and k is the free space wave vector.

The reflected field is calculated on a plane, which is perpendicular to the axis of the beam. In contrast to simpler methods the Physical Optics solver also considers mode conversion effects due to non-perpendicular incidence on the mirror as well as a small cross polarised component, which is generated when straight field lines are reflected by a curved mirror surface.

2.2 FFT Propagation

For the free space propagation after the last mirror, an FFT-based algorithm is used. It is based on the fact, that the Fourier transform of a spatial field distribution is equivalent to a spectrum of plane waves, which propagate under different angles. After passing a distance d , each of these waves is multiplied with a phase factor, which corresponds to the k -component in the main propagation direction. The spatial field distribution can then be obtained with an inverse FFT. To ensure the maximum speed and accuracy, the forward transform is only applied to the initial field and the inverse transform is calculated for each point, where the field is of interest.

Since the 2D Fourier transform implies, that the field distribution is periodic in x - and y -directions, some artefacts can occur in the propagated field, which are interferences from the virtual neighbour beams. They

can be avoided by padding the field with zeros, which increases the FFT-size and thus the calculation time.

2.3 Gaussian beam analysis

To compare the simulated results with design values or results from other software packages, the beam profiles, which are available only numerically, need to be fitted to Gaussian beam parameters. This is done with a multidimensional optimizer, which was already used successfully for different optimization tasks [5].

In each iteration, the fitting routine generates a synthetic Gaussian beam and calculates the overlap integral with the given field pattern. From this, the power fraction of higher order modes can be calculated. The optimizer varies the Gaussian beam parameters such, that the power of the higher modes becomes as small as possible. Start values for the beam parameters are obtained by analysing the field pattern and calculating some statistical parameters. From a field pattern, the following parameters can be obtained:

- The position of the beam centre
- The angle of the beam axis with respect to the z -axis of the coordinate system
- The ellipse radii
- The ellipse orientation

For beams with a simple astigmatism it is also possible to obtain the positions and radii of the beam waists. The beams in this paper, however, have a general astigmatism, which was not supported by PROFUSION, when the analysis was done (see section 4.1).

2.4 Tracking of the polarisation

As mentioned above, the linear polarisation in the resonance should be vertical (i.e. in z -direction of the global torus coordinate system). In order to determine the correct polarisation vector in the launcher, a tool was written, which tracks the polarisation over a sequence of mirrors. For one reflection on one mirror, the relevant vectors are shown in Fig. 4.

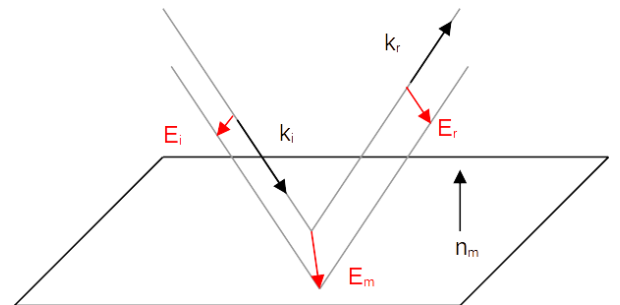


Fig. 4. E-field vectors for a reflection on a flat mirror

The incident beam has a wave vector k_i and an electrical field vector E_i . Both vectors define the *polarization plane* of the beam. The simple rule is that the polarisation planes of the incident and reflected beams intersect the mirror plane in the same line, which is

equivalent to the E-field vector E_m projected onto the mirror.

Mathematically the following formalism can be used to calculate E_r . Note that the lengths of the vectors are not relevant here and are assumed to be normalised. Also, the sign of the vector products does not need to be considered, because a multiplication with -1 results only in an inverted phase but keeps the polarisation unchanged.

The normal vector n_i of the polarisation plane of the incident beam is:

$$\vec{n}_i = \vec{E}_i \times \vec{k}_i \quad (3)$$

The projected field E_m on the mirror can then be calculated with the normal vector n_m of the mirror:

$$\vec{E}_m = \vec{n}_i \times \vec{n}_m = (\vec{E}_i \times \vec{k}_i) \times \vec{n}_m \quad (4)$$

Together with the wave-vector k_r of the reflected beam the normal vector n_r of the polarisation plane of the reflected beam becomes:

$$\vec{n}_r = \vec{E}_m \times \vec{k}_r = ((\vec{E}_i \times \vec{k}_i) \times \vec{n}_m) \times \vec{k}_r \quad (5)$$

Finally, the electric field vector E_r can be calculated from n_r and k_r

$$\vec{E}_r = \vec{n}_r \times \vec{k}_r, \quad (6)$$

which leads to the following expression for E_r :

$$\vec{E}_r = (((\vec{E}_i \times \vec{k}_i) \times \vec{n}_m) \times \vec{k}_r) \times \vec{k}_r \quad (7)$$

Note that n_m can be calculated using the reflection law from k_i and k_r . This means that the only necessary parameters for a sequence of mirrors are the incident and reflected wave vectors and the direction of the initial E-vector.

Ideally the field vector in the resonance should be in X-mode, which corresponds to the z -direction of the global torus coordinates. This condition can, however, be fulfilled only approximately, because the field vector is always perpendicular to the k -vector (in an isotropic medium) and the latter is slightly tilted with respect to the x - y -plane (i.e. the equatorial plane of the vessel). The best physically possible E-direction was obtained by defining an auxiliary vector a , which is perpendicular to the k -vector and lies in the x - y plane:

$$\vec{a} = \begin{pmatrix} 0 \\ 0 \\ 1 \end{pmatrix} \times \vec{k}_{res} \quad (8)$$

The best possible E-vector E_{res} then becomes:

$$\vec{E}_{res} = \vec{a} \times \vec{k}_{res} \quad (9)$$

From this field vector, the described method was applied in backwards direction to get the E-vector at the exit of the waveguides in the upper launcher. This vector was then used to do the full simulation with the physical optics solver in forward direction.

3 Simulation Framework

All solvers are part of the PROFUSION code package [4], which was developed over more than two decades and contains a large number of routines tools for microwave optics, both for free space and in waveguides.

The PROFUSION tools are commandline programs, which are written in C and run on Linux computers. This has the advantage that a calculation is fully defined by the data files (if needed) and the command line. This improves the reproducibility and allows to control even complex simulations (e.g. including parameter scans) by simple shell scripts. PROFUSION also contains a large number of small tools for doing standard calculation (like 3D vector arithmetic, coordinate transformations, evaluation of mathematical expressions), which make it possible to convert the parameters obtained from IO to the values needed by the solvers. The calculation scheme works basically as follows:

- Use redundant parameters provided by the ITER Organization (IO) to make some consistency checks
- Transform the parameters from the ones provided by IO to the ones used by the solvers where necessary
- Run the solvers to calculate the field patterns
- Run the analysis to obtain the Gaussian parameters and other data
- Generate the field plots

Since we always start with the data provided by ITER, potential errors from manual conversion could be avoided.

The most time-consuming routine is the physical optics solver, which calculates the output field in a 2D plane according to Eq. (2), which results in 4 nested loops. Therefore, it was parallelized to run on multiple CPU cores (up to 40 on the available machines). In addition, different beams could be calculated by different servers in parallel. This made it possible to simulate a whole set of beams (U or L) including the analysis in a few hours. During the project, the PROFUSION tools were upgraded with some new features, most notably:

- Support for mirrors with irregular (i.e. numerically given) boundaries
- Support for passing all coordinates in an arbitrary global coordinate system (TGCS in the ITER case).
- Determination of the ellipse rotation angle of the Gaussian fit tool
- Implementation of a tool for tracking the polarisation across a sequence of mirrors with Eq. (7)
- A tool for generating discretized datasets of mirror surfaces from geometry parameters (cylinder, ellipsoid or hyperboloid).

4 Results

4.1 Field patterns

The fields reflected by the mirrors were calculated at different reference position, which were chosen such, that they are as close as possible to the following mirror without the field plane intersecting the mirror surface.

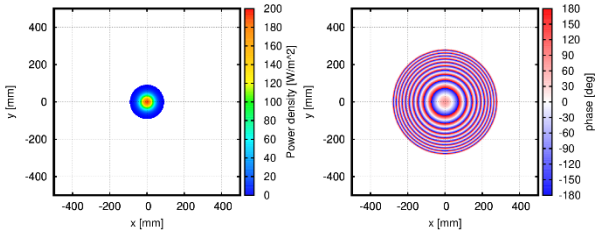


Fig. 5. Field of the beam U1 after the mirror M2 in the upper launcher.

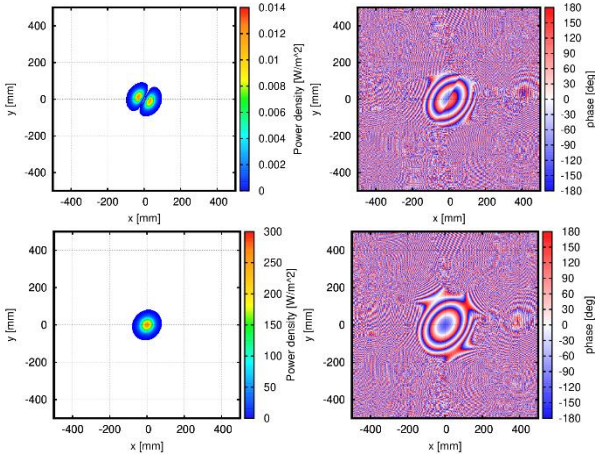


Fig. 6. Field of the beam U1 after the Mirror M3. Left: Power density in W/m^2 for a 1 W beam, right: Phase in degrees.

Fig. 5 shows the initial field of the beam U1 between M2 and M3 in the upper launcher, which is a circular Gaussian beam. The left image shows the power density of the field in W/m^2 for a total beam power of 1 W, which is the standard normalization in PROFUSION. The right image shows the phase in degrees. Fig. 6 shows the fields of U1 after the mirror M3. The upper images show the cross polarization, the lower image shows the main polarization. The coordinate systems for the field plots after M3 are chosen such, that the y-axis is aligned to the main polarization direction, which is required for a maximum power in the X-mode polarization. Therefore, the very small cross polarization becomes visible. For a beam power of 1 MW the power in the cross polarization is less than 0.05% and is considered uncritical since the only effect is a slightly decreased heating efficiency.

Figure 7 shows the field of the beam U1 after the mirror M4. Figure 8 shows the field of U1 after the mirror UA. Some stray radiation is visible especially in the cross polarization, which comes from beam truncation due to the limited size of the mirror UA. It will further be analysed in section 4.3. The effect also occurs for the co-polarised component, but it is invisible in the field plot due to the different scale.

The beams have a general astigmatism [6], where the amplitude and phase ellipses are not aligned.

Furthermore, the amplitude ellipse changes its orientation along the propagation axis. Such beams can be described with a complex rotation angle of the ellipse, which was not supported by PROFUSION at the time the analysis was done. Therefore, the beam phase was set to zero before the analysis and the most important parameters, the ellipse radii, were determined by assuming a flat phase front.

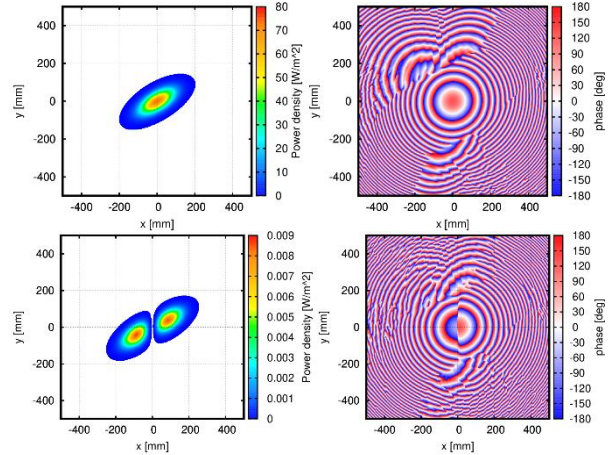


Fig. 7. Field of the beam U1 after the mirror M4

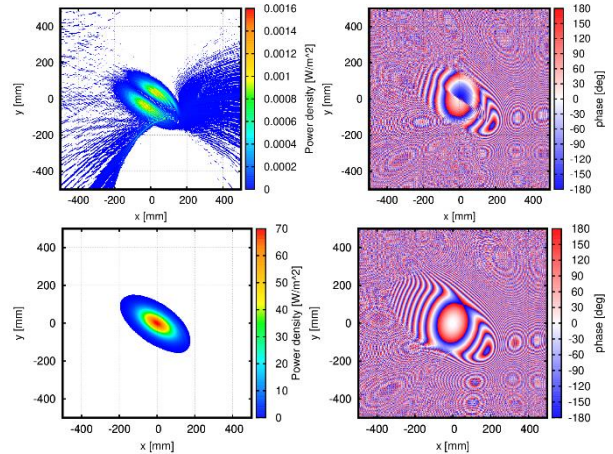


Fig. 8. Field of the beam U1 after the mirror UA

4.2 Beam profiles

The profiles of the U1-beam are shown in Fig. 9. They are plotted over a distance of 7 m from the last reference plane, which includes the way through the resonance. The z-axis in Fig. 9 is the beam axis. Again, we see a slight disturbance coming from the truncation by the mirror UA. It is, however, very small in terms of spurious mode power and only visible in a logarithmic plot.

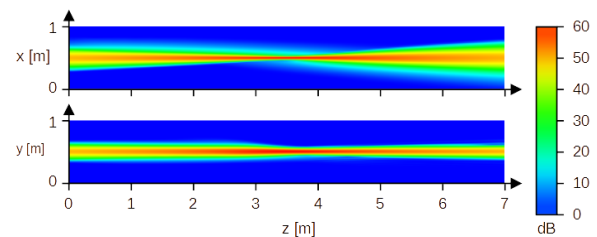


Fig. 9. Horizontal (top) and vertical (bottom) profiles of the U1 beam after the mirror UA

The power density, which is relevant for the plasma breakdown and the heat load in the beam dump, is shown in Fig. 10. It is, again, the power density along the beam axis in W/m^2 for a total beam power of 1 W.

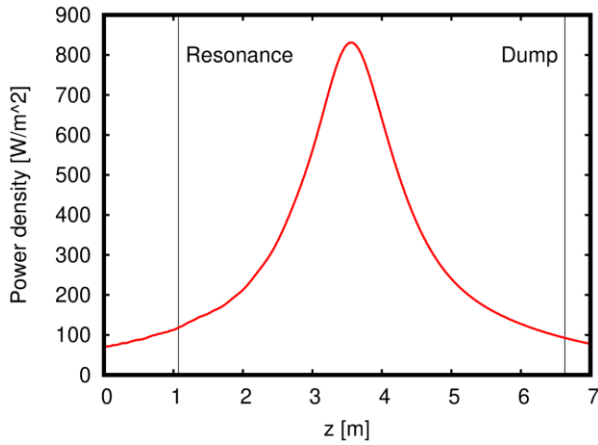


Fig. 10. Power density at the axis of the U1 beam after the mirror UA for a total beam power of 1 W.

4.3 Beam truncation by the mirror UA

The physical optics solver allows to handle the beam truncation by a limited mirror size by simply assuming the surface currents to be zero for points outside the mirror contour. Together with a routine for the point-in-polygon problem, it is possible to consider irregular mirror contours, which are given in terms of a polygon.

The most critical situation is the beam U1 on the mirror UA. The mirror UA is located very close to the plasma and therefore needs to be as small as possible. Fig. 11 shows the beam footprint on the mirror and the mirror contour.

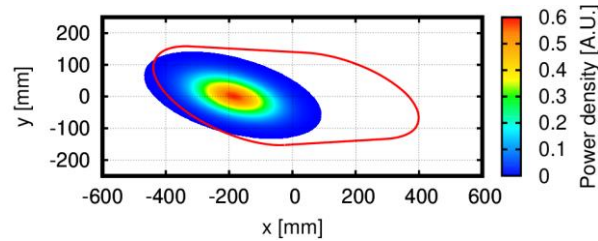


Fig. 11. Footprint of the beam U1 on the mirror UA. The contour is shown in red

With the current configuration the power outside of the mirror is 0.48 %. To estimate the effects of the spill-over on sensitive in-vessel components, the field outside of the mirror contour was calculated (Fig. 12) and propagated by 100 mm (Fig. 13) to estimate the power density near the vessel wall. Note that the coordinate system of Fig. 11 is a mirror-local system of UA, the coordinate system of Figs 12 and 13 is a beam-local coordinate system of the beam U1.

The estimated power density was checked against the coordinates of some sensitive in-vessel components, which are located near UA and no critical values could be identified.

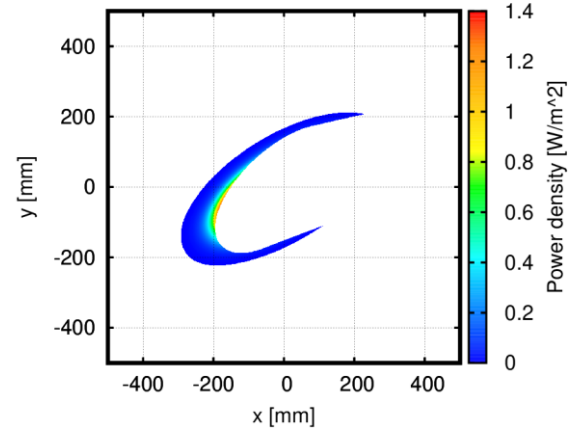


Fig. 12. Spill-over power of the beam U1 in the plane of the mirror UA.

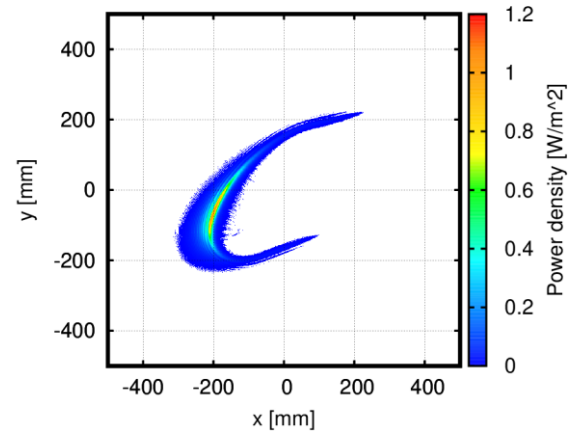


Fig. 13. Spill-over power of the beam U1 100 mm behind the plane of the mirror UA.

4.4 Comparison with the design values

To verify the calculation, the positions of the beam centres were calculated with the Gaussian fit tool (see section 2.3) and compared with the design values (obtained with the Catia software). Table 1 shows the result for the U-beams at the location of the beam dump. At this location the beam passed 3 mirrors and more than 13 m of free space propagation, so the errors are expected to be the largest there.

We can see a very good agreement. The maximum error is 1.702 mm, which is much smaller than the minor beam radius (57.309 mm) and therefore negligible compared to other expected errors, e.g. from spurious waveguide modes.

Table 1. Coordinates (in mm) of the U-Beams in the beam dump

Beam	Reference	Calculation	Error [mm]
U1	9397.991	9398.183	0.870
	-5614.515	-5614.194	
	277.215	278.000	
U2	9523.528	9523.031	1.702
	-5387.328	-5388.469	
	252.132	253.293	
U3	9639.352	9639.284	1.014
	-5174.561	-5174.834	
	220.869	221.843	

5 Comparison with raytracing

In parallel to the PROFUSION simulation, the system was simulated with the commercial Zemax OpticStudio software. Fig. 14 shows the field of the beam U2 after the mirror UA calculated with PROFUSION and Zemax.

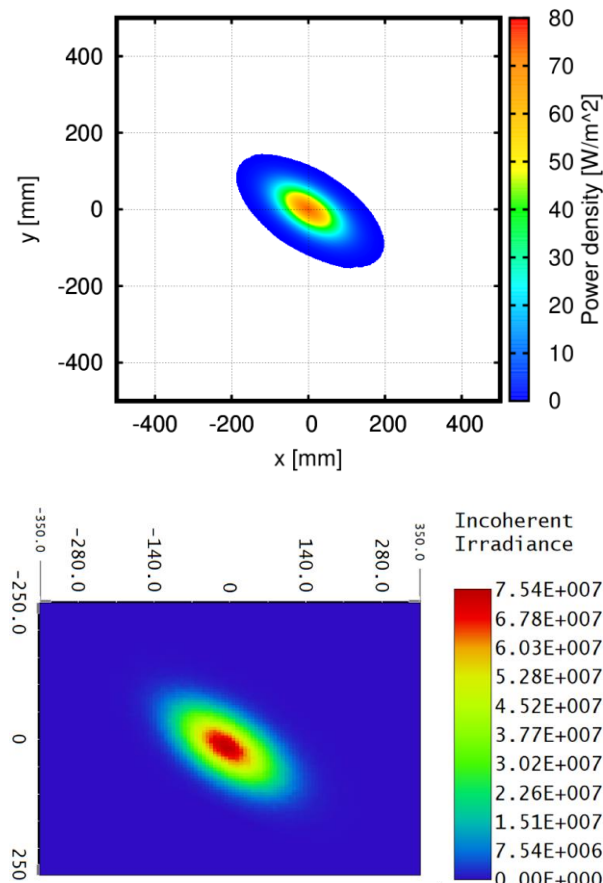


Fig. 14. Field of the beam U2 after the mirror UA calculated with PROFUSION (top) and Zemax (bottom)

We can see a good agreement of the shape and orientation of the beam ellipse. Furthermore, the peak value of the field (which is 73.6 W/m^2 for the PROFUSION result) is in reasonable agreement. The factor of approximately 10^6 is due to the fact, that the PROFUSION result is for a beam power of 1 W, while the Zemax calculation is for 1 MW.

6 Modifications of the system

During the project, some modifications of the system were suggested by ITER and the simulation was re-run. Due to organizational issues and the ending of the contract, a comprehensive analysis of the modified design could not be done but is planned for the future. All results presented in this paper are for the initial design, where all necessary data is available.

7 Conclusion

The simulation and analysis of the in-vessel optics for the first ITER plasma could verify both a feasible design

and the accuracy as well as the flexibility of the simulation framework, which was built around the PROFUSION tools.

The design fulfils the requirements in terms of minimum power density in the resonance and maximum power density in the beam dump. The most critical component is the mirror UA, which has a limited size due to its position near the plasma and suffers from a small fraction of the power reaching the vessel wall and a truncation of the reflected beam. A detailed analysis using the coordinates of sensitive in-vessel components could not identify any critical issues, also the effects of the beam truncation on the reflected beam are uncritical.

Comparisons with the initial design of the U-beams and raytracing calculations with Zemax showed a very good agreement.

This work was funded by the ITER organization under the service contract No. 43-2080.

References

1. D. Strauss et.al., *Nearing final design of the ITER EC H&CD Upper Launcher*, Fusion Engineering and Design **146**, 2019, 23–26, <https://doi.org/10.1016/j.fusengdes.2018.11.013>
2. F. Fanale et.al., *Design validation of in-vessel mirrors and beam dump for first plasma operations in ITER*, Fusion Engineering and Design, **172**, 2021, 112717, ISSN 0920-3796, <https://doi.org/10.1016/j.fusengdes.2021.112717> .
3. A. Moro, et al., *Design of Electron Cyclotron Resonance Heating protection components for first plasma operations in ITER*, Fusion Engineering and Design, 154, 2020, 111547, ISSN 0920-3796, <https://doi.org/10.1016/j.fusengdes.2020.111547> .
4. B. Plaum, *Simulation of microwave beams with PROFUSION*, 2019 Edition, <http://dx.doi.org/10.18419/opus-10252>
5. B. Plaum, *Optimization of Broadband Smooth-Wall Circular Horn Antennas*. J Infrared Milli Terahz Waves 39, 984–995 (2018). <https://doi.org/10.1007/s10762-018-0510-6>
6. J. A. Arnaud and H. Kogelnik, "Gaussian Light Beams with General Astigmatism," Appl. Opt. 8, 1687-1693 (1969)